

## Article

# Design of a Prototypical Mock-Up for the Experimental Investigation of WCLL First-Wall Performances

Pietro Maccari , Pietro Arena , Ranieri Marinari , Amelia Tincani  and Alessandro Del Nevo 

ENEA, Department for Fusion and Technology for Nuclear Safety and Security, C.R. Brasimone, 40032 Camugnano, Italy

\* Correspondence: [pietro.maccari@enea.it](mailto:pietro.maccari@enea.it)

**Abstract:** A large research effort is currently ongoing within the framework of the EUROfusion consortium for the study and design of a water-cooled lithium–lead (WCLL) breeding blanket (BB). This concept will be tested in ITER through the installation of a test blanket module (TBM) and it is one of the two candidates adopted as driver BBs in DEMO. In this framework, at the ENEA research centre of Brasimone, the realization of the experimental platform, W-HYDRA, is envisaged. The platform is dedicated to the support of the development of WCLL BB and ITER TBM and the investigation of the DEMO balance of plants. One of the most important experimental infrastructures is the water-loop facility, the aim of which is to provide water at a high pressure and temperature (PWR conditions), with a sufficient mass-flow rate and power for the experimental testing of BB and TBM components. The facility will be equipped with a vacuum chamber and an electron beam gun for the reproduction of high surface heat flux on plasma-facing components. In the present work, the design of a prototypical mock-up (MU) of the WCLL BB first wall is described. The MU is used to investigate the thermal, hydraulic and structural behavior of the current first-wall design under relevant heat loads at the expected operational conditions. The delineation of the main experimental test's features and the instrumentation needed is assessed in the paper. A preliminary CFD calculation on the prototypical MU and the computational results are also presented.

**Keywords:** DEMO; WCLL breeding blanket; water loop; CFD; first wall; mock-up



**Citation:** Maccari, P.; Arena, P.; Marinari, R.; Tincani, A.; Del Nevo, A. Design of a Prototypical Mock-Up for the Experimental Investigation of WCLL First-Wall Performances. *Energies* **2023**, *16*, 1685. <https://doi.org/10.3390/en16041685>

Academic Editor: Rob J.M. Bastiaans

Received: 10 January 2023  
Revised: 28 January 2023  
Accepted: 4 February 2023  
Published: 8 February 2023



**Copyright:** © 2023 by the authors. Licensee MDPI, Basel, Switzerland. This article is an open access article distributed under the terms and conditions of the Creative Commons Attribution (CC BY) license (<https://creativecommons.org/licenses/by/4.0/>).

## 1. Introduction

The WCLL BB is one of the most promising BB concepts currently under development for DEMO reactors [1–3]. Its water-cooled first wall (FW) consists of a EUROFER steel structure, cooled by squared channels, which was designed for the removal of high heat loads in the expected operational conditions of the DEMO. For the proper qualification of this component and the investigation of its cooling capabilities, an experimental campaign to be carried out at the ENEA Brasimone research centre is planned. In the framework of these experiments, a FW mock-up (MU) is planned to be tested under relevant operating conditions. In particular, the foreseen water loop (WL) facility [4] will provide pressurized water under the WCLL BB's operational conditions, while the expected plasma heat fluxes (HFs) will be applied by means of an electron-beam gun (EB gun) similar to that used in [5]. The experiments will have to provide relevant information regarding the suitability of the WCLL FW for future use in a DEMO reactor. Similar studies were recently carried out in the HELOKA helium facility at KIT, for the helium-cooled pebble bed (HCPB) blanket concept [6,7].

Due to the complexity of the BB layout and the heat loads expected during its operation, the representativity of the MU with respect to the reference FW presents some challenges. For this reason, the development of the MU layout and of the experimental test matrix should be accurately developed, starting from the scientific objectives and requirements of each test.

In the present paper, a preliminary FW MU layout is presented, within the context of its integration in the WL facility. Thermal loads relevant to the DEMO were applied to the MU by the EB gun, which was included in the experimental apparatus. Based on this design, a first numerical study aiming at the reproduction of the relevant cooling conditions for FW channels by the MU is presented. The investigation began with the Ansys-CFX-code simulation of the FW in normal steady-state operational conditions. The results of the reference simulation were used to set up the MU experimental-test boundary conditions and to conduct a comparison against the pre-test simulation of the MU in experimental conditions. Beyond describing the design of the experimental layout developed for the FW characterization campaign, the objective of this paper is to present the heating-system design and the approach adopted for the repartition of the thermal loads on the MU structure. The goal of the set-up is the reproduction of relevant thermal–hydraulic conditions in the water-cooling channels of the MU, which is the main requirement for the investigation of FW cooling capability in experimental conditions.

## 2. The Water-Loop Facility of the W-HYDRA Infrastructure

The water-thermal-hydraulic (W-HYDRA) infrastructure is an experimental platform that is to be built at the Research Centre of ENEA Brasimone. It will include three main facilities: WL, STEAM and LIFUS5/Mod4 [4]. The WL is a medium-scale water facility that will provide a test bed for the WCLL BB, with the possibility of hosting test sections/mock-ups for the investigation of different phenomena and components. In addition, it will be applied as a platform for the testing of the water-cooling system of the ITER WCLL TBM at full scale, as well as offering the ability to test the thermal–hydraulic and thermo-mechanic performances of high heat fluxes (HF)-heated components. For this specific purpose, the facility will be equipped with a vacuum chamber hosting an 800-kilowatt EB gun. Table 1 reports the main hydraulic features of the WL, while the general layout of the facility is shown in Figure 1.

**Table 1.** The WL facility's main parameters.

Working Fluid	Water
Working-temperature range	110–328 °C
Design temperature	350 °C
Nominal pressure	15.5 MPa
Design pressure	18.5 MPa
Nominal mass-flow rate	3.74 kg/s

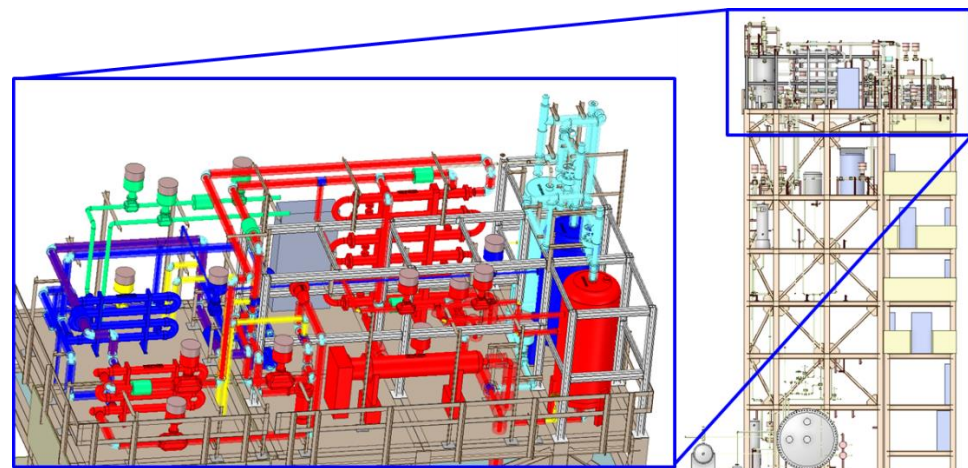


**Figure 1.** Overall view of WL facility and its supporting structure (red: primary loop; blue: secondary loop; green: tertiary loop).

The facility is mainly constituted by three loops:

1. A primary water loop with the main goal of supplying water in PWR conditions at the different test sections, equipped with an electric heater of 800 kW.
2. A secondary water loop with the aim of reproducing the secondary loop of the WCLL–TBM circuit, whose main function is to avoid in any case the injection of radioactive water into the ITER component cooling water system (CCWS).
3. A tertiary water loop acting as a final heat sink for the WL. In the case of the WCLL–TBM, this circuit plays the role of the ITER CCWS.

### 3. Prototypical FW–MU Layout and Objectives of the Experimental Campaign

The first step in the design of the prototypical FW–MU and the set-up of the experimental test matrix is the definition of the scientific objectives to be achieved in the campaign. These can be summarized in three main points:

- Test the thermal–hydraulic performances of the FW under relevant working conditions, at full scale.
- Test the deformations of the FW under relevant working conditions and the thermal fatigue resistance under relevant cyclic working conditions, at full scale.
- Provide experimental data for the assessment and validation of numerical codes.

Each point can be further divided into more detailed objectives, from which the requirements to be met by the MU and the specifics of the experimental campaign can be defined. The present study is focused on the first point, related to the characterization of the thermal–hydraulic performances of the FW.

#### 3.1. FW–MU Thermal–Hydraulic–Characterization Campaign

The FW–MU thermal–hydraulic–characterization campaign includes the following sub-objectives:

- Measuring the temperatures reached in the solid structure of the FW under relevant conditions.
- Investigating the cooling capability of the FW channels (the power exported by the water up to the critical heat flux (CHF) conditions) under relevant conditions.
- Investigating the incipience of the water boiling in the FW channels and of the different boiling regimes under relevant conditions.
- Investigating the effect of gravity and buoyancy forces on the cooling capability of the FW by considering different channel inclinations.
- Measuring the pressure drops in the FW channels under relevant conditions.

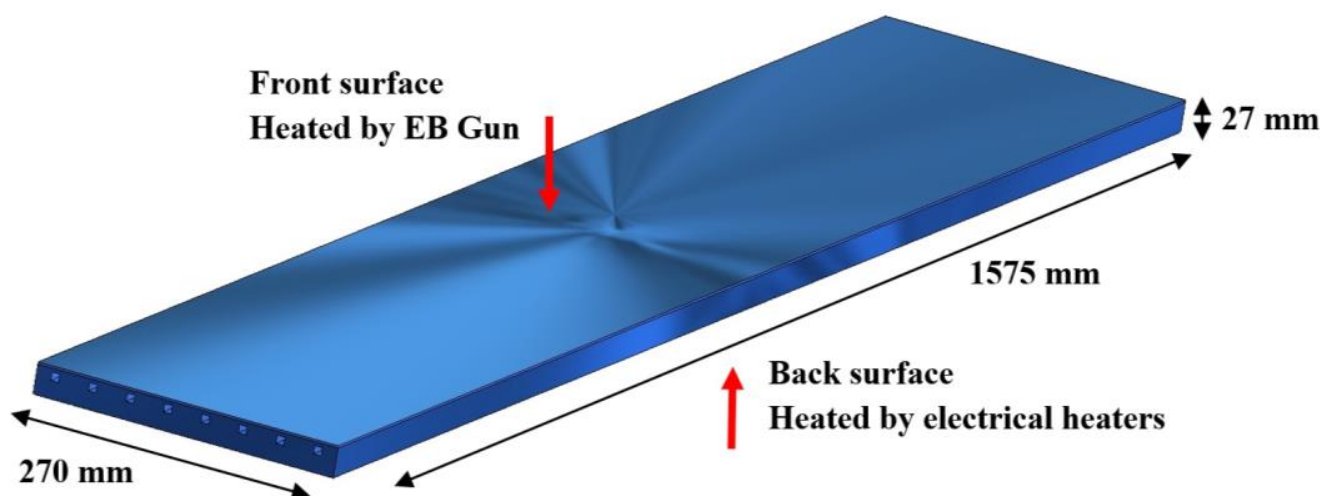
The relevant conditions include both nominal operating conditions (steady-state and normal-operation transient) and relevant accidental transient conditions.

#### 3.2. The MU Geometry

The first preliminary MU design investigated is intended to satisfy most of the requirements for the fulfillment of the objectives described above. Considering the complexity of the real FW layout, a simplification of the structure was needed to maintain acceptable manufacturing and operational costs. For this purpose, the considered MU design is a flat structure intended to reproduce at full scale a section of the plasma-facing FW. To this end, the four-channel cooled FW of the central outboard blanket (COB) segment of the BB [3] was considered as the reference design. According to the dimensions reported in Table 2, the MU reproduces two adjacent COB units in the poloidal (vertical) direction and it features the same radial thickness and channel geometry as the FW. In the toroidal direction, the MU was given the same total length as the plasma-faced FW, calculated by summing the extensions of the flat and the two bent parts. Indeed, the so-called side walls (SW) were not expected to receive any HF from the plasma. The manufacturing materials will be chosen to be as close as possible to Eurofer steel in terms of material properties. An overview of the MU geometry with the main quotes is presented in Figure 2.

**Table 2.** Main dimensions of the FW–MU.

Thickness (radial direction)	25 mm (+2 mm of tungsten coating)
Height (poloidal direction)	270 mm
Length (toroidal direction)	1575 mm
Front-heated surface	0.42 m <sup>2</sup>
Channel pitch	33.75 mm
Sides of squared channels	7 mm
Channel distance from heated surface	5 mm
Number of cooling channels	8

**Figure 2.** FW–MU layout and dimensions.

### 3.3. Experimental Set-Up and Diagnostics

Cooling water at nominal reference conditions of 15.5 MPa and 295 °C is provided to the MU through the connection to the WL facility. The HF mimicking that coming from the plasma is applied on the front surface of the MU by means of the 800-kilowatt EB gun. In addition, electrical heaters are planned to be installed to heat up the MU back surface, reproducing the FW heat exchange with the breeding zone (BZ).

In Figure 3, a preliminary piping-and-instrumentation diagram (P&ID) of the MU and its connection with the WL facility is presented. In the diagram, bulk fluid temperature thermocouples are denoted as TC, wall-temperature thermocouples are denoted as TW, differential pressure (DP) meters are denoted as DP and pipes are denoted as P. The water from the WL is split into two lines, feeding the FW–MU from opposite sides. Next, a couple of manifolds are used to uniformly split the mass flows coming from the two main branches into 4 lines each, connected to the 8 MU squared channels. Cooling water flows in the MU channels in a counter current. The 8 outlet lines gather in a collector to a single outlet line stretching back to the WL.

The 2 main inlet lines from the WL can be operated by means of a pneumatic valve and a manual (isolation) valve in order to impose the same flow rate on the two branches (under normal operational conditions) or to simulate coolant-maldistribution scenarios (e.g., LOFA scenario).

Thermocouples for the bulk-fluid-temperature measurement are located on the two main inlet lines, on the output line and on 8 MU outlet pipes, as shown in Figure 3. The DP meters will be positioned across 3 MU channels. On the same channels, there 9 bulk-fluid-temperature thermocouples are placed per channel, uniformly distributed along the length of the MU. In addition, 18 thermocouples are inserted in the MU structure, between

two consecutive channels, to measure the internal temperature of the structure during tests (see Figure 3). The accurate mapping of the temperature in the MU is also used for the validation of numerical codes.

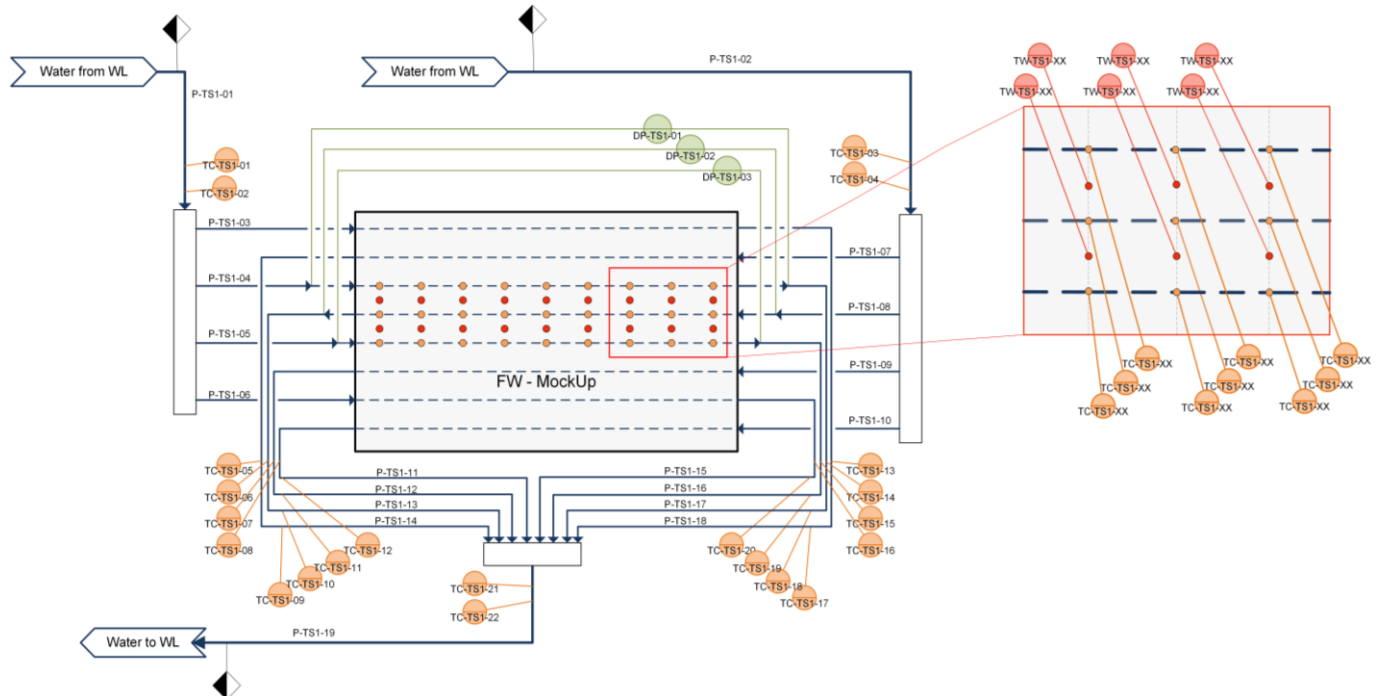


**Figure 3.** Pipe-and-instrumentation Diagram of the FW-MU.

In addition, the following diagnostic equipment is used:

- An infrared camera and pyrometers to monitor the surficial temperature on the EB-gun-heated surface.
- Accelerometer equipment to monitor the boiling conditions in the MU channels.

#### 4. CFD Analysis and Validation of the Prototypical MU Design

With respect to the scientific objectives listed in Section 3.1, it should be highlighted that some major challenges threaten the representativeness of the MU with respect to the reference FW and, thus, the production of relevant results for the FW validation in the experimental tests. From the thermal-hydraulic point of view, these challenges can be summarized through the following points:

- The neutronic (volumetric) deposited heat power cannot be reproduced in the MU.
- Power exchange with the BZ is non-uniformly distributed along the poloidal abscissa of the BB segment, since it depends on both the volumetric deposited heat power and the positioning of the double-wall tubes near the FW.
- The MU is characterized by its different geometry (no bents) and reproduces only a part of the whole FW. However, this should be an acceptable simplification, since no HF is deposited onto the external surfaces of the neglected areas.

Accordingly, in view of the envisaged experimental campaign finalized by testing the FW thermal-hydraulic performances, the aim of the CFD analysis reported below is to investigate the applicability of the MU layout to the achievement of the presented scientific objectives. In particular, with a focus on points 2 and 3 of the objectives listed in Section 3.1, the goal of the analysis is to investigate the possibility of reproducing representative thermal-hydraulic conditions in the water-cooling channels with the envisaged MU experimental apparatus. The simulation results will be useful for the design and sizing



of some experimental components (e.g., electrical heaters, etc.) and for the set-up of the experimental-test matrix.

#### 4.1. Set-Up of Reference FW Simulation

The reference FW conditions are represented by the COB elementary cell at equatorial level (V0.6 B model [8]) during normal steady-state operation. This BB element is characterized by the highest neutronic power and the lowest plasma HF; therefore, it features the most challenging heat loads for the MU to be representative.

A CFD simulation of a COB elementary cell (FW and BZ domains) was carried out by applying the reference water-boundary conditions and reference heat loads (i.e., neutronic power, plasma HF) considering the most recent available neutronic calculations [9]. A fine mesh was used in the simulation by imposing a value of  $y^+ = 1$  to the inflation control near the solid walls for the resolution of the viscous sub-layer in all the water domains. The total number of mesh nodes was about 32 million and the total number of elements was about 57 million. The calculation was carried out with the Ansys-CFX code by using the  $k-\omega$  shear-stress-transport-turbulence model. The main boundary conditions considered in the simulation are reported in Table 3. The power-load distribution in the front part of the FW (i.e., toroidal and bent parts of FW) is reported in Table 4.

**Table 3.** Main boundary conditions used in the the FW reference simulation (COB in normal steady-state operational conditions).

FW water total mass-flow rate	0.632 kg/s
BZ water total mass-flow rate	1.262 kg/s
Water inlet T (both FW and BZ)	295 °C
Water P (both FW and BZ)	15.5 MPa
Plasma HF on FW [10]	HF function of toroidal coordinate. Max value: 320 kW/m <sup>2</sup>
Neutronic power [9]	Volumetric heat-power function of radial coordinate

**Table 4.** Power-load repartition in the front part of the FW.

	Power (kW)	Power %
Power of plasma HF	64.97	53.07
Power exchanged with BZ	15.65	12.78
Neutronic power	41.82	34.16
Total	122.42	100

The thermo-physical properties of water, Pb–Li, Eurofer and Tungsten were implemented in the CFX code as constants or temperature-dependent functions using a polynomial fitting of data. The properties of the solid domains are specified in terms of density, specific heat and thermal conductivity, while the fluid domain also requires dynamic viscosity.

The calculation results of interest for the set-up of the MU test is the power removal of FW channels. The results of the simulation are summarized in Section 4.3, along with the simulation results of the MU.

#### 4.2. Set-Up of MU Experimental Test Simulations

The results of the reference FW CFD simulation (Section 4.1) were used as a starting point to set-up the boundary conditions to be adopted in the simulation of the MU experimental test, with the aim of obtaining conditions as similar as possible in the cooling channels of the MU. The water pressure and mass-flow rates (boundary conditions) selected were the same as those in the reference FW case; the inlet water temperature in the channels was set at 296.6 °C, as it was the average channel temperature at the inlet of the first bent

of the FW in the reference simulation. Regarding the heat loads, a criterion was adopted in order to split the reference total power (Table 4), including the volumetric heat power, between the two HFs available in the MU (i.e., the EB gun on the front surface and the heaters on the back surface). With the aim of obtaining the greatest possible similarity in the water conditions within the cooling channels, the power of the two applied HFs was obtained by means of an iterative procedure, in which the goal was to meet the following two criteria:

- The sum of the two applied powers (i.e., EB-gun power and back-heater power) must be equal to the total power of the reference FW simulation (122.4 kW per elementary cell).
- The ratio between the power removed by the front sides of the cooling channels and that removed by the back sides has to be the same as the reference FW calculation ( $P_{\text{channels\_front}}/P_{\text{channels\_back}} = 1.557$ ).

As a result of the iterative procedure, the total power to be applied on the front surface of the MU (EB gun power) was 92.45 kW (per elementary cell); the total power applied to the back surface of the MU was 29.89 kW (per elementary cell). The main boundary conditions of the MU are summarized in Table 5. The non-heated surfaces of the MU were considered adiabatic. The same code, models and mesh size were set up in the CFD calculation with respect to the reference simulation. In this case, the total number of mesh nodes was about 14.2 million and the total number of elements was about 13.6 million

**Table 5.** Main boundary conditions used in the MU simulation (steady-state).

MU water total mass-flow rate (per elementary cell)	0.63189 kg/s
Water inlet T	296.6 °C
Water P (both FW and BZ)	15.5 MPa
Front HF distribution	Maximum value of 454 kW/m <sup>2</sup> , reaching zero at the borders (in the toroidal direction) with a sinus function
Back HF distribution	Uniform value of 142 kW/m <sup>2</sup>
Power applied on front surface (per elementary cell)	92.45 kW
Power applied on back surface (per elementary cell)	29.89 kW

#### 4.3. Results of MU Simulation Compared with Reference FW Simulation

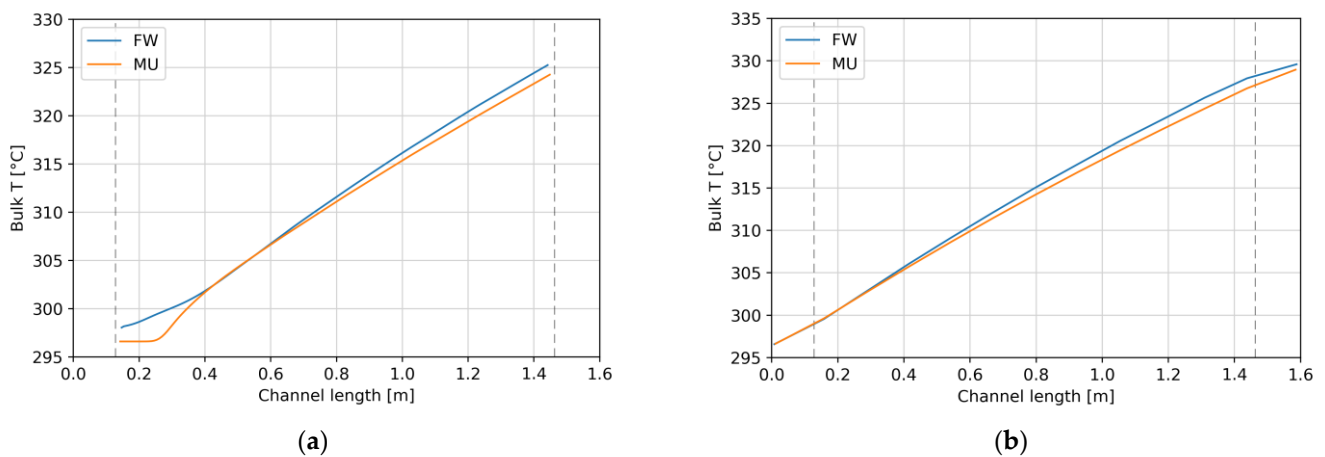
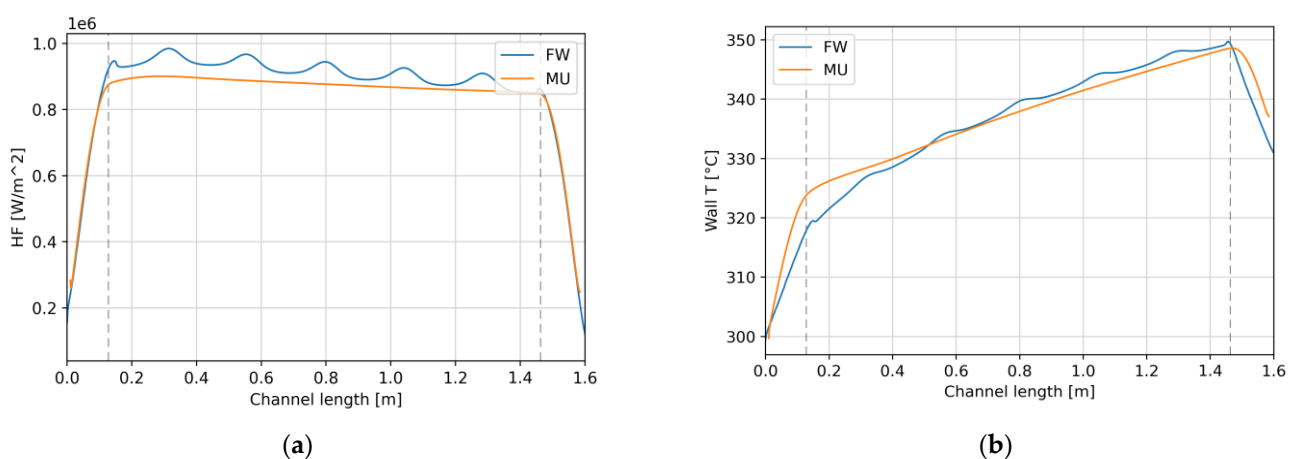
Both the CFD simulations converged well with all the residuals reducing below  $10^{-6}$ , which means that the steady-state results had good accuracy. In the comparison, attention was focused on the thermal–hydraulic parameters describing the water domains in the squared channels, removing power by convection and conduction from the hot surrounding solid domain. Accordingly, a key point is the heat transfer through the interface surfaces between the solid and liquid domains (squared channel sides).

A first general comparison can be assessed by examining the power repartition on the front (plasma-faced), back (BZ-faced) and lateral sides of the squared channels. It has been reported in Table 6. for both the FW and the MU calculations results. It can be observed that similar heat loads were obtained with the adopted criterion on the four channel faces. The main difference is that the power removed by the lateral sides of the channels was slightly higher for the MU and, consequently, the power removed from both the front- and the back-channel sides was higher in the FW case. The average water-outlet temperature in the MU was uniform in the 8 channels and consistent with the reference FW value at the outlet of the bent part (around 329 °C).

**Table 6.** Power repartition on the sides of the squared channels in the FW and the MU simulations.

Channels Side	FW Power (kW)	FW Power %	MU Power (kW)	MU Power %
Front sides	39.65	32.40	38.03	31.11
Back sides	25.32	20.70	24.43	19.98
Lateral sides	57.38	46.90	59.78	48.90
Total	122.40	100	122.23	100

To obtain more information on the representativity of the channels' cooling conditions, some plot comparisons along a reference channel were reported for the MU and the FW. Figure 4a shows the water temperature at the channel center and Figure 4b shows the bulk temperature (mass-flow average in the channel section) along the straight part of the FW channel. In Figure 5a, the wall-to-liquid HF on the top-side center of a reference channel is reported and Figure 5b shows the wall temperature along the front-side center of a reference channel.

**Figure 4.** Channel-center temperature (a) and bulk temperature (b), along the length of a reference channel.**Figure 5.** Wall-to-liquid HF (a) and wall temperature (b) along the front-side-wall center of a reference channel.

Along the bent parts of the FW channel, an increase in the turbulence enhancing the water mixing in comparison to the straight MU channel, was expected. For this reason, a slightly higher wall temperature was observed in the first 30 cm of MU channels (Figure 5b) and, correspondingly, a slightly higher temperature was reached in the center



of the FW channel (Figure 4a). A similar behavior was observed in the outlet bent of the channel, where the wall temperature dropped faster in the FW than in the MU (Figure 5b). Along the straight part of the FW, the slightly higher power removal obtained in the FW case (see Table 6) suggests a slightly faster increase in the temperature both on the wall and in the fluid bulk (Figures 4 and 5).

An oscillation of the variables plotted along the FW channels can be observed in Figure 5. This was due to the influence of the heat exchange with the BZ, which, as explained above, varied along the toroidal abscissa due to the presence of the double wall tubes (DWTs).

In general, a good match between the plotted variables was obtained between the MU and the FW simulations, meaning a good representativity of the cooling channels in the studied steady-state conditions by the MU. Figure 6 depicted the wall temperature along the sides of the channels for the two simulations, while Figure 7 reports the temperature field in a vertical central section of the reference channel, in the water domain. In both cases, a very similar thermal field can be observed, but the effects of the bends-turbulence enhancement on the fluid field can also be observed in the FW temperature distribution in Figure 7.

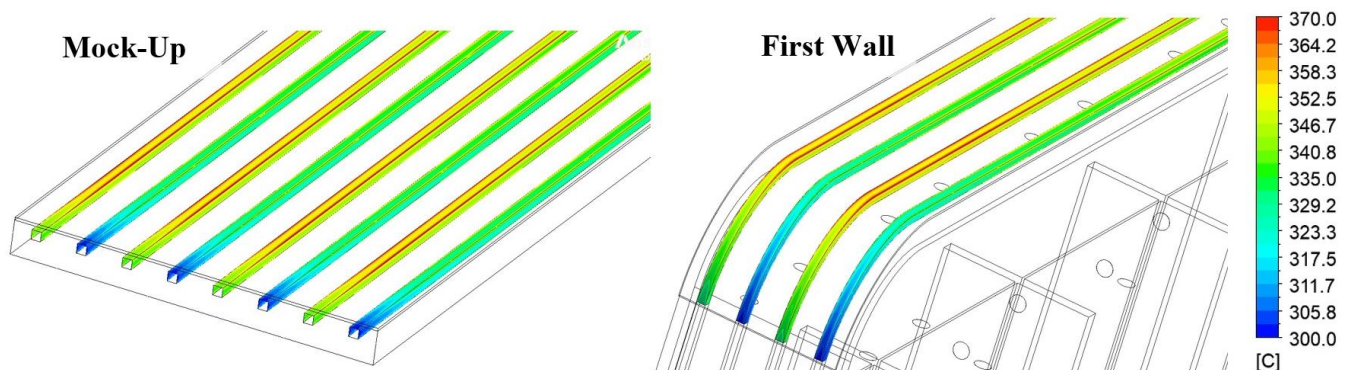


Figure 6. Wall temperature along the channel sides for the FW and the MU.

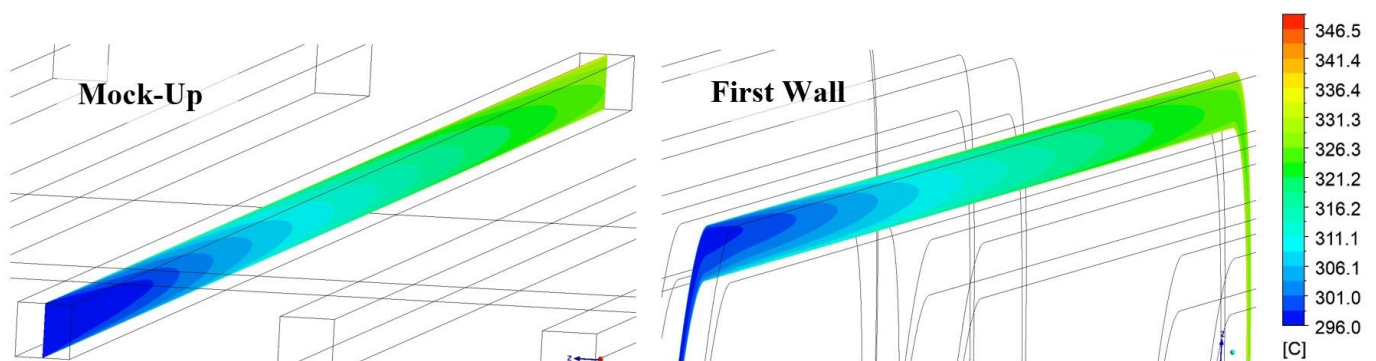


Figure 7. Temperature field in a vertical central section of the reference channel fluid.

Some additional observations regarding the thermal field obtained in the structures should be examined (Figure 8). The different distributions of power applied and, in particular, the higher boundary HFs applied to the MU (to compensate for the absence of the neutronic load) led to the achievement of higher temperatures in the MU structures in comparison to the FW reference scenario. Consequently, it has to be considered that experimental activities aiming at the characterization of the mechanical behavior of the FW may be influenced by this mismatch.

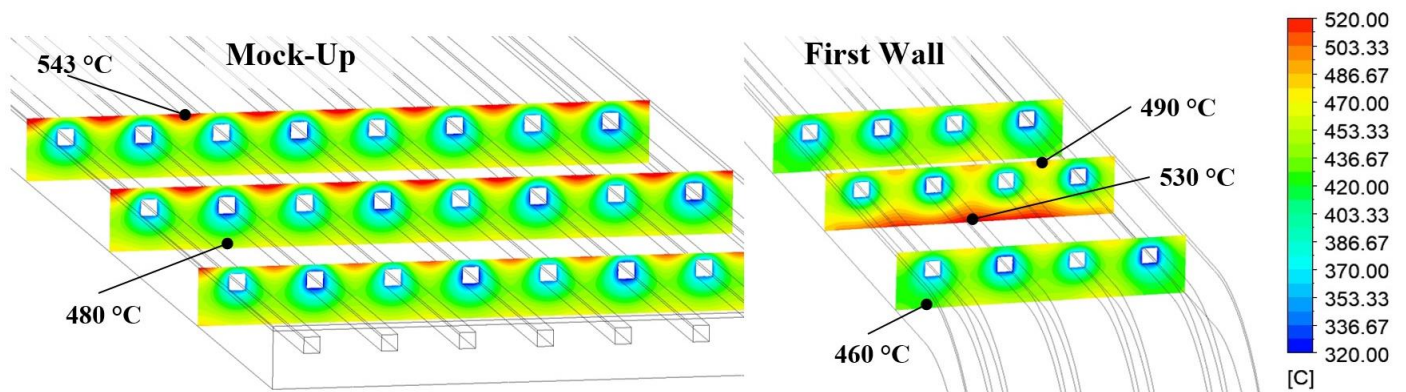


Figure 8. Structure-temperature field for the FW and MU simulations.

## 5. Conclusions

In view of the envisaged experimental campaign intended to provide relevant information for the validation of the FW component of the WCLL BB, a prototypical FW–MU was proposed for manufacturing and testing in the WL experimental facility within the W-HYDRA infrastructure. The prototypical MU geometry, the experimental apparatus and the diagnostic instrumentation were presented in this paper, according to the first preliminary design conceived.

Due to the complexity of the reference FW geometry and operational conditions, the representativity of the MU in prototypical experimental conditions must be investigated in order to produce relevant results in the envisaged experimental campaign. Therefore, given the MU layout, the representativity of its thermal–hydraulic conditions with respect to the reference FW were numerically assessed in the present paper. In this regard, the first step was the CFD simulation of the COB elementary cell of the FW at the equatorial level in normal steady-state operational conditions, from which relevant FW heat loads were estimated.

The simulation results for the reference FW were used to set up the HF boundary conditions for the MU, using a criterion intended to obtain representative thermal–hydraulic conditions in the water-cooling channels.

The comparison of the FW simulation results with the MU simulation results shows a good reproduction of the overall power repartition between the cooling-channel sides. The plot comparison of the thermal–hydraulic variables along the length of a reference channel also featured a good match between the cooling conditions. Moreover, these plots underline the effect of the bent part of the FW, which increases the heat exchange between the wall and the fluid, leading to some discrepancies. Further sensitivity studies on this phenomenon should be conducted to better quantify the effects of the bends on the heat transfer of the channels. A slightly different thermal field was predicted for the FW–MU with respect to the WCLL BB FW. Nevertheless, the proposed FW–MU can be used for the investigation of the mechanical behavior of the FW under selected loading conditions.

In conclusion, it can be stated that, despite some discrepancies compared with the reference model, the designed MU and its projected heating system fulfil the experimental test objectives set. Indeed, with the adopted thermal loads, it features representative thermal–hydraulic conditions in the cooling channels. Consequently, its design and the investigated thermal loads can be used as a starting point for the development of the experimental test matrix. Future experimental testing will deal with the investigation of the channels' cooling conditions, the investigation of the water nucleate boiling phenomenon and a test of the thermo-mechanical performances under cyclic loads.

**Author Contributions:** Conceptualization, P.M., P.A., A.T. and A.D.N.; methodology, P.M., P.A., R.M. and A.D.N.; software, P.M. and R.M.; validation, P.A. and R.M.; formal analysis, P.M. and P.A.; investigation, P.M. and R.M.; resources, P.A., A.D.N. and A.T.; data curation, P.M., P.A. and R.M.; writing—original draft preparation, P.M. and R.M.; writing—review and editing, P.A., R.M., A.D.N. and A.T.; visualization, P.M. and R.M.; supervision, P.A. and A.D.N.; project administration, P.A., A.T. and A.D.N.; funding acquisition, A.D.N. and P.A. All authors have read and agreed to the published version of the manuscript.

**Funding:** This work was carried out within the framework of the EUROfusion Consortium, funded by the European Union via the Euratom Research and Training Programme (grant agreement no. 101052200—EUROfusion).

**Data Availability Statement:** Data sharing is not applicable to this article.

**Acknowledgments:** This work was carried out within the framework of the EUROfusion Consortium, funded by the European Union via the Euratom Research and Training Programme (grant agreement no. 101052200—EUROfusion). The views and opinions expressed are, however, those of the author(s) only and do not necessarily reflect those of the European Union or the European Commission. Neither the European Union nor the European Commission can be held responsible for them.

**Conflicts of Interest:** The authors declare no conflict of interest.

## Abbreviations

BB	Breeding Blanket
BZ	Breeding Zone
CCWS	Component Cooling Water System
CHF	Critical Heat Flux
COB	Central Outboard Blanket
DP	Differential Pressure
DWT	Double Wall Tube
EB Gun	Electron Beam Gun
FW	First Wall
HF	Heat Flux
HCPB	Helium-Cooled Pebble Bed
LOFA	Loss Of Flow Accident
MU	Mock-Up
P&ID	Piping-and-Instrumentation Diagram
SW	Side Walls
TBM	Test-Blanket Module
WCLL	Water-Cooled Lithium–Lead
WL	Water Loop
W-HYDRA	Water-Thermal-Hydraulic

## References

1. Federici, G.; Bachmann, C.; Barucca, L.; Biel, W.; Boccaccini, L.; Brown, R.; Bustreo, C.; Ciattaglia, S.; Cismonti, F.; Coleman, M.; et al. DEMO design activity in Europe: Progress and updates. *Fusion Eng. Des.* **2018**, *136*, 729–741.
2. Boccaccini, L.V.; Arbeiter, F.; Arena, P.; Aubert, J.; Bühler, L.; Cristescu, I.; Del Nevo, A.; Eboli, M.; Forest, L.; Harrington, C.; et al. Status of Maturation of Critical Technologies and Systems Design: Breeding Blanket. *Fusion Eng. Des.* **2022**, *179*, 113116.
3. Arena, P.; Del Nevo, A.; Moro, F.; Noce, S.; Mozzillo, R.; Imbriani, V.; Giannetti, F.; Edemetti, F.; Froio, A.; Savoldi, L.; et al. The DEMO Water-Cooled Lead–Lithium Breeding Blanket: Design Status at the End of the Pre-Conceptual Design Phase. *Appl. Sci.* **2021**, *11*, 11592.
4. Del Nevo, A.; Arena, P.; Eboli, M.; Lorusso, P.; Tincani, A.; Badodi, N.; Cammi, A.; Giannetti, F.; Ciurlini, C.; Forgione, N.; et al. The design of Water Loop facility for supporting the Water Coolant Lithium Lead Breeding Blanket technology and safety. In Proceedings of the 32nd SOFT, Dubrovnik, Croatia, 18–23 September 2022.
5. Weber, T.; Bürger, A.; Dominiczak, K.; Pintsuk, G.; Banetta, S.; Bellin, B.; Mitteau, R.; Eaton, R. Improvements in electron beam monitoring and heat flux flatness at the JUDITH 2-facility. *Fusion Eng. Des.* **2015**, *96*, 187–191.
6. Ghidersa, B.E.; Ionescu-Bujor, M.; Janeschitz, G. Helium Loop Karlsruhe (HELOKA): A valuable tool for testing and qualifying ITER components and their He cooling circuits. *Fusion Eng. Des.* **2006**, *81*, 1471–1476.

7. Zeile, C.; Abou-Sena, A.; Boccaccini, L.V.; Ghidersa, B.E.; Kang, Q.; Kunze, A.; Lamberti, L.; Maione, I.A.; Rey, J.; von der Weth, A. Conceptual design of a First Wall mock-up experiment in preparation for the qualification of breeding blanket technologies in the Helium Loop Karlsruhe (HELOKA) facility. *Fusion Eng. Des.* **2016**, *109*, 1335–1339.
8. Edemetti, F.; Di Piazza, I.; Del Nevo, A.; Caruso, G. Thermal-hydraulic analysis of the DEMO WCLL elementary cell: BZ tubes layout optimization. *Fusion Eng. Des.* **2020**, *160*, 111956.
9. Arena, P.; Del Nevo, A.; Moro, F.; Noce, S.; Mozzillo, R.; Imbriani, V.; Giannetti, F.; Edemetti, F.; Froio, A.; Savoldi, L.; et al. Design and integration of the EU-DEMO Water-Cooled Lead Lithium Breeding Blanket. In Proceedings of the 32nd SOFT: 32nd Symposium on Fusion Technology, Dubrovnik, Croatia, 18–23 September 2022.
10. Maviglia, F.; Bachmann, C.; Federici, G.; Franke, T.; Siccino, M.; Albanese, R.; Ambrosino, R.; Arter, W.; Bonifetto, R.; Calabrò, G.; et al. Integrated design strategy for EU\_DEMO first wall protection from plasma transients. *Fusion Eng. Des.* **2022**, *177*, 113067.

**Disclaimer/Publisher’s Note:** The statements, opinions and data contained in all publications are solely those of the individual author(s) and contributor(s) and not of MDPI and/or the editor(s). MDPI and/or the editor(s) disclaim responsibility for any injury to people or property resulting from any ideas, methods, instructions or products referred to in the content.